Monitoring of shrinkage and creep of concrete using fibre Bragg grating sensors

Author/Contributor:
Wong, Allan; Childs, Paul; Peng, Gang-Ding; Gowripalan, Nadarajah

Publication details:
5th International Conference on Optical Communications and Networks & the 2nd International Symposium on Advances and Trends in Fiber Optics and Applications
pp. 480-483
7811142643 (ISBN)

Event details:
5th International Conference on Optical Communications and Networks & the 2nd International Symposium on Advances and Trends in Fiber Optics and Applications
Chengdu & Jiuzhaigou, China

Publication Date:
2006

DOI:
https://doi.org/10.26190/unsworks/639

MONITORING OF SHRINKAGE AND CREEP OF CONCRETES USING FIBRE BRAGG GRATING SENSORS

*Allan C. L. Wong[1], Paul A. Childs[1], N. Gowripalan[2] and Gang-Ding Peng[1]**
[1]School of Electrical Engineering and Telecommunications, University of New South Wales, Sydney NSW 2052, Australia
[2]School of Civil and Environmental Engineering, University of New South Wales, Sydney NSW 2052, Australia

ABSTRACT

Fibre Bragg grating (FBG) sensors are used for the experimental investigation of two of the most important time-dependent properties of concrete: drying shrinkage and creep. A swept wavelength system is used as the interrogation technique. The FBG sensors are embedded directly into structural grade concrete specimens. Standard mechanical method is used in parallel with the embedded FBG sensors. Both mechanically and optically measured time-dependent strains are discussed. It is shown that the FBG sensors offer a better alternative to the conventional electrical and mechanical methods, in the measurement of long-term time-dependent strains.

Keywords: *Fibre Bragg grating, concrete, shrinkage, creep, strain*

1. INTRODUCTION

Experimental investigation of the time-dependent properties of concrete: drying shrinkage and creep, are of practical importance, as many significant long-term characteristics are being affected by these two factors. Shrinkage is the time-dependent strain measured in an unloaded and unrestrained concrete specimen, and it occurs principally due to the loss of water during the drying process, known as drying shrinkage. Creep is the time-dependent increase in the strain of concrete under a sustained compressive or tensile stress. Creep is in some ways affected by similar factors to shrinkage, as they are both affected by the hydration, drying and the time-dependent change of the hardened cement paste. Drying shrinkage, in particular, is responsible for the cracking, structural deformation and deflection, and other detrimental effects in concrete structures that lead to serviceability and durability failures. Although in many situations creep relieves high stresses, it may also lead to structural deformation [1].

Fibre Bragg grating (FBG) sensors combine many advantages from both the electrical and mechanical methods: (i) they have high strain resolution; (ii) they provide better long-term stability and do not drift with time; (iii) they are immune to electromagnetic interference; (iv) they are not affected by moisture; (v) they can be multiplexed easily and conveniently along a single optical fibre link; (vi) they have the capability of taking measurements automatically, continuously, and remotely from the measuring locations; (vii) they can be installed into the concrete structure either by embedding or surface-mounting; and (viii) they have compact and small size that, in most cases, are non-perturbative to the test structure. Thus, they are well suited for the monitoring of time-dependent effects and physical behaviour of the body of the concrete structure.

In this paper, the application of FBG sensors to concrete technology is demonstrated. Specifically, the drying shrinkage and creep of structural grade (20 – 50 MPa) concrete are measured using embedded FBG sensors. In accordance with the Australian Standards, mechanical method is also performed in parallel with the optical method. The former method measured the core strain of the concrete specimens, whereas the latter method measured the surface strain. The results obtained from both methods are discussed.

**Corresponding author. E-mail: G.Peng@unsw.edu.au*

2. FBG SENSING TECHNIQUE

2.1 Sensing principle

A FBG is specified by the Bragg wavelength, i.e., $\lambda_B = 2n_{eff}\Lambda$, where n_{eff} is the effective refractive index and Λ is the grating period. The shift in the λ_B due to strain (ε) and temperature (T) changes is given by [2],

$$\Delta\lambda_B = (1 - p_e)\lambda_B\Delta\varepsilon + (\alpha + \xi)\lambda_B\Delta T\,, \qquad (1)$$

where $p_e = (n^2/2)[P_{12} - \mu(P_{11} + P_{12})] \approx 0.22$ is the effective photo-elastic coefficient, P_{ij} are the Pockels coefficients of the strain-optic tensor and μ is the Poisson's ratio. $\alpha = (d\Lambda/dT)/\Lambda$ is the coefficient of thermal expansion, and $\xi = (dn_{eff}/dT)/n_{eff}$ is the thermal-optic coefficient. The λ_B-shift is influenced by both the strain and thermal changes of the grating region. Since all experiments were performed in a controlled room at constant temperature (T = 23 ºC), the second term in Eq. (1) can be discarded. Furthermore, the following assumptions are made in the measurements: (i) the debonding and slippage of interfaces between the fibres and concrete specimens are negligible [3-5]; and

(ii) the grating region and the fibres as a whole do not suffer from deterioration and damage [6].

2.2 Sensor fabrication

FBG sensors were fabricated at our grating writing facility with different λ_B's using the direct phase-mask technique. The sensors were annealed at 300 °C in order to increase the long-term stability, and were re-coated with polymer material (acrylate) to protect against mechanical and corrosive damages from the highly alkaline (pH = 13) concrete material.

2.3 Sensor system setup

A swept-wavelength system (SWS) was used for the sensor interrogation and strain measurements, and the setup is depicted in Fig. 1. It comprised a C-band tuneable laser connected to the embedded FBG sensors through a 3-dB fibre coupler. The laser constantly scans a wide wavelength range and when the wavelength is matched to the λ_B, a large resonant signal is reflected back and passed to a photodetector module. The reflected signal is then processed by a computer, and by tracking the shift in the λ_B, the strain value is obtained. This interrogation method can yield a strain resolution of 1 με. The crosstalk is negligible provided the λ_B-peaks of the sensors do not overlap with each other. Since the SWS is a passive interrogation system that does not involve interferometric methods or high-frequency moving parts; it does not suffer from large static drift and the need for frequent re-calibration. Thus, this is a preferred technique for the measurement of long-term time-dependent strains of concrete.

3. CONCRETE SPECIMEN PREPARATION

The concrete mix was prepared and cast into two type of moulds (rectangular prism and cylinder) according to the Australian Standards AS 1012.2 and AS 1012.8.1 [7]. The mix composed of cement, sand, coarse aggregate (gravel with a maximum particle size of 19 mm) and water, and had a water-to-cement (w/c) ratio of 0.57. The rectangular prism had dimensions of 75 × 75 × 280 mm^3, and the cylinder had dimensions of 100 mm in diameter and 200 mm in height. Before casting, FBG sensors were inserted and placed into positions in the moulds as shown in Fig. 2. For the prisms, the sensors were inserted horizontally at the centre of the moulds and kept parallel to the longitudinal axis by stretching both ends while casting the concrete mix. The lead-in and lead-out fibres projected out on the surface near the ends of the prisms. For the cylinders, the sensors were placed vertically at the centre of the cylinder moulds and aligned in the direction of loading. Two small loops were wrapped on both sides of the grating regions, so that both lead-in and lead-out fibres were projected out on the side wall of the moulds. The fibres had to exit from the side of the cylinders as the compressive load was applied on both ends when performing the creep

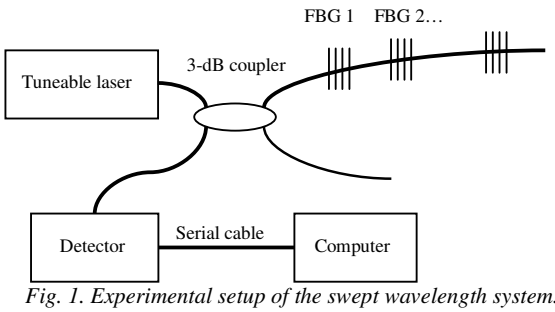

Fig. 1. Experimental setup of the swept wavelength system.

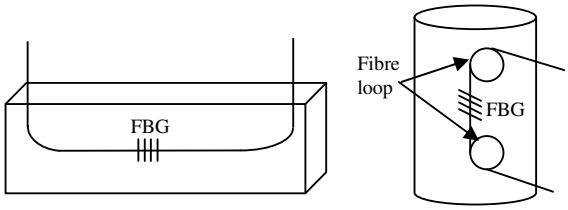

Fig. 2. Method of embedding FBG sensors into specimens.

experiment. The specimens were initially cured and demoulded after 24 hours from moulding, and then stored in a fog room with standard moist curing conditions (T = 23 °C and relative humidity (RH) = 100 %) to age 7 days. After that they were transported and kept in a drying room with standard drying conditions (T = 23 °C and RH = 50 %) for subsequent drying shrinkage and creep experiments.

4. DRYING SHRINKAGE

The drying shrinkage experiment of concrete prisms was performed in accordance with the Australian Standard AS 1012.13 [8]. Optical measurements of the strain of the prisms were obtained from the embedded FBG sensors. A length comparator together with a 295 mm reference bar was used to measure the actual fractional length change of the prisms. The length comparator has a resolution of 0.002 mm or about 7.1 με. Fig. 3 shows the drying shrinkage of the concrete prisms obtained by optical and mechanical measurements. The first reading was taken at an age of 7 days from casting. As can be seen from Fig. 3, the drying shrinkage strain increased rapidly within the first few days, and then increased more gradually afterwards. At the beginning, both methods gave similar shrinkage, but deviated progressively with time. The difference in the measured shrinkage strains became almost constant after 2 weeks, with the difference being about 100 με. The drying shrinkage strain from the mechanical measurement was always larger than the optical measurement, indicating that the surface of the prisms shrank more than that in the core. Depending on the size and thickness of the structure, core and surface strains differ because of the differences in the moist condition, capillary transportation of water content and redistribution of internal stress throughout the structure. Drying shrinkage is due largely to the evaporation of water from the prism,

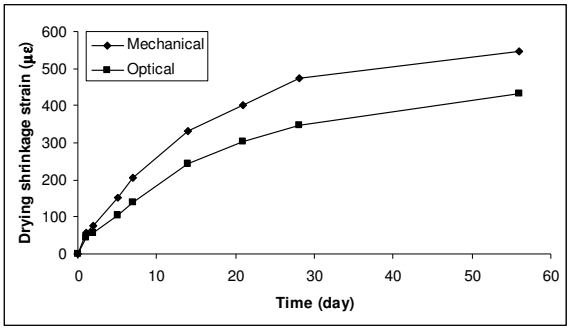

Fig. 3. Drying shrinkage of concrete prisms.

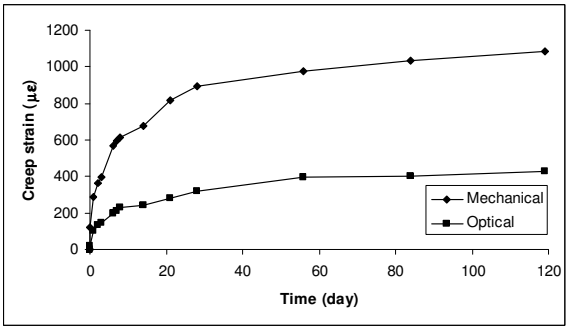

Fig. 5. Creep of concrete cylinders after loading.

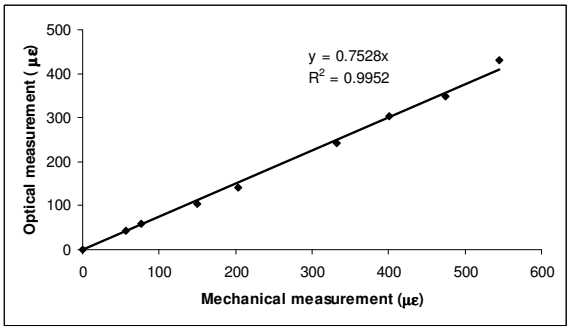

Fig. 4. Relationship between optical and mechanical measurements of drying shrinkage strain of concrete prisms.

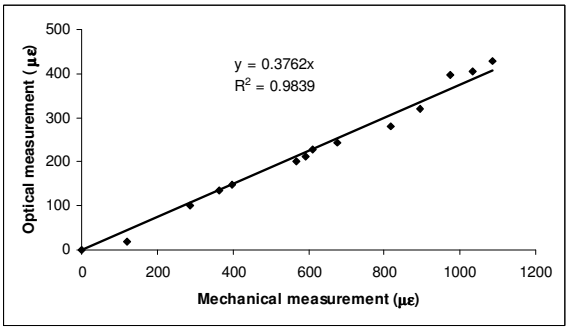

Fig. 6. Relationship between optical and mechanical measurements of creep strain of concrete cylinders.

and the drying conditions of the ambient environment. The degree and rate of drying vary throughout the depth of the prism. The portion of the prism, notably at the surface, that is exposed to the ambient environment experienced the greatest and fastest amount of shrinkage. On the other hand, at the core of the prism, since the water required a longer time to be transported to the surface via the pores, the shrinkage was smaller and slower than that at the surface. Although there was a difference in the shrinkage strain measured between the two methods on the prism, the difference is small as expected. The two measurements are more comparable as measured along the axis of the prism, and their shrinkage growth trends were remarkably similar. Fig. 4 shows the relationship between the optical and mechanical measurements of drying shrinkage strains. They yielded a very high degree of correlation, indicating that both measurements agreed very well, with the difference being only 100 με.

5. CREEP

5.1 Creep strain

At the age of 28 days from moulding, the compressive strength of the concrete was tested, and a value of 40 MPa was obtained. The creep experiment was performed in accordance with the Australian Standard AS 1012.16 [9]. Two cylinders with embedded FBG sensors were loaded in a hydraulic pressurised creep rig with 40 % of the concrete strength, i.e., 16 MPa of compressive load. Two companion unloaded cylinders were placed in the same drying room, which were used to obtain the drying shrinkage strain. Mechanical measurement was obtained by using a demountable mechanical strain gauge (Demec), which has a resolution of 0.002 mm or 16.2 με. Optical measurement was obtained from the embedded FBG sensors, similar to the prior drying shrinkage experiment.

Fig. 5 shows the creep strain of the concrete cylinders obtained from optical and mechanical measurements. The first reading was taken immediately after loading, at the age of 28 days from moulding. The creep strain was determined from the total strain taken directly from the loaded cylinders, and subtracting the instantaneous elastic strain and drying shrinkage strain taken from the companion unloaded cylinders. The creep strain increased rapidly in the first week after loading, and became more stable after 1 month. The difference in the creep strain between the optical and mechanical measurements was about 700 με after 120 days of loading, which is considered large. The high degree of correlation between the optical and mechanical methods can be seen in Fig. 6.

5.2 Total strain

The total strain ε_T of a concrete specimen under a constant and sustained compressive load is given by [1],

$$\varepsilon_T = \varepsilon_{ins} + \varepsilon_{crp} + \varepsilon_{shr} + \varepsilon_{thm}, \qquad (2)$$

where ε_{ins} is the instantaneous elastic strain, ε_{crp} is the creep strain, ε_{shr} is the drying shrinkage strain, and ε_{thm} is

the thermal strain. The instantaneous elastic strain can be determined by measuring the strain immediately after a load is applied. The creep strain measured from the loaded cylinder consists of both the creep and drying shrinkage strains. The drying shrinkage strain can be separately measured from a companion unloaded cylinder under the same environmental condition as the loaded cylinder. The thermal strain can be discarded if the temperature is kept constant, which was the case in our experiments.

The total strain of the concrete cylinders under a compressive load is shown in Fig. 7. The first reading was taken before loading, at the age of 28 days from moulding. The average instantaneous elastic strain for a compressive load of 16 MPa was 402 με and 616 με from the optical and mechanical measurements, respectively. The behaviour of the creep strain (including the creep and drying shrinkage strain) is shown in the figure as subsequent data points after the onset of the instantaneous elastic strain. Thus, the total strain curve gives the complete history of the time-dependent behaviour of the loaded cylinders. Again, besides the strain difference, the high degree of correlation and agreement between the optical and mechanical measurements can be seen in Fig. 8.

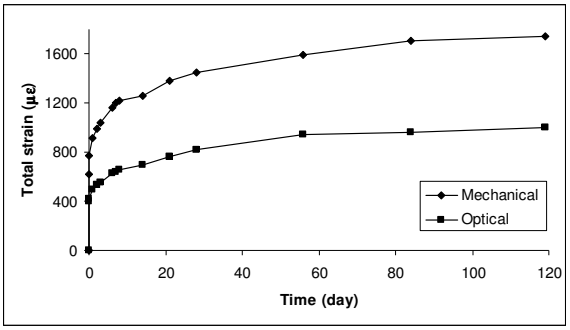

Fig. 7. Total strain of concrete cylinders under a sustained compressive load.

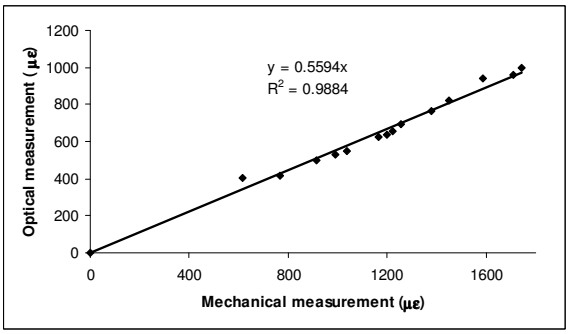

Fig. 8. Relationship between optical and mechanical measurements of total strain of concrete cylinders.

6. CONCLUSIONS

The drying shrinkage and creep strains of structural grade concrete were measured and investigated using the embedded FBG sensors. The results were compared and analysed with the standard mechanical method using the length comparator and the Demec. The embedded FBG sensors yielded a very high degree of correlation with the mechanical method. The FBG sensors combine many advantages of the electrical and mechanical methods, notably they can be embedded directly into the wet concrete with minimal interference with the structure. The capability of multiplexing a large number of sensors in series along a single optical fibre link, as well as taking measurements automatically and remotely from the measuring locations, are the unique advantage of this type of fibre-optic sensors. Thus, the FBG sensors offer a better alternative to the conventional methods of long-term strain measurement of concrete.

7. ACKNOWLEDGEMENTS

The authors thank William Terry for assistance in the concrete preparation. This work was supported by the Australian Research Council and the Roads and Traffic Authority, NSW, Australia, under a Linkage grant.

8. REFERENCES

[1] R.I Gilbert, "Time effects in concrete structures", Elsevier, Amsterdam (1988)

[2] A.D. Kersey *et al*, "Fiber Grating sensors", J. Lightwave Technol. **15**, pp1442-1463 (1997)

[3] F. Ansari and Y. Libo, "Mechanics of bond and interface shear transfer in optical fiber sensors", J. Eng. Mech. **124**, pp385-394 (1998)

[4] C.K.Y. Leung, X. Wang and N. Olson, "Debonding and calibration shift of optical fiber sensors in concrete", J. Eng. Mech. **126**, pp300-307 (2000)

[5] Q. Li *et al*, "Elasto-plastic bonding of embedded optical fiber sensors in concrete", J. Eng. Mech. **128**, pp471-478 (2002)

[6] W.R. Habel and H. Polster, "The influence of cementitious building materials on polymeric surfaces of embedded optical fibers for sensors", J. Lightwave Technol. **13**, pp1324-1330 (1995)

[7] Standards Australia, AS 1012.2, "Preparation of concrete mixes in the laboratory" (1994); and AS 1012.8.1, "Method for making and curing concrete – Compression and indirect tensile test specimens" (2000)

[8] Standards Australia, AS 1012.13, "Determination of the drying shrinkage of concrete for samples prepared in the field or in the laboratory" (1992)

[9] Standards Australia, AS 1012.16, "Determination of creep of concrete cylinders in compression" (1996)